

SIMULATION OF POROSITY AND PTFE CONTENT IN GAS DIFFUSION LAYER ON PROTON EXCHANGE MEMBRANE FUEL CELL PERFORMANCE

NUR H. MASLAN¹, MARVIN M. GAU², MOHD S. MASDAR²,
MASLI I. ROSLI^{2,*}

¹Fuel Cell Institute, Universiti Kebangsaan Malaysia, 43600 UKM Bangi, Selangor, Malaysia

²Department of Chemical and Process Engineering, Faculty of Engineering and Built Environment, Universiti Kebangsaan Malaysia, 43600 UKM Bangi, Selangor, Malaysia

*Corresponding Author: masli@ukm.edu.my

Abstract

Numerous research and development activities have been conducted to optimize the operating parameters of a proton exchange membrane fuel cell (PEMFC) by experiments and simulations. This study explains the development of a 3D model by using ANSYS FLUENT 14.5 to determine the optimum PEMFC parameters, namely, porosity and polytetrafluoroethylene (PTFE) content, in the gas diffusion layer (GDL). A 3D model was developed to analyze the properties and effects of GDL. Simulation results showed that the increase in GDL porosity significantly improved the performance of PEMFC in generating electrical power. However, the performance of PEMFC decreased with increasing PTFE content in GDL. Thus, the PTFE content in the GDL must be optimized and the optimum PTFE content should be 5 wt%. The model developed in this simulation showed good capability in simulating the PEMFC parameters to assist the development process of PEMFC design.

Keywords: Proton exchange membrane fuel cell, Gas diffusion layer.

1. Introduction

Hydrogen energy is a green energy source that has high potential to replace oil, coal, and natural gas. A fuel cell, in particular a proton exchange membrane fuel cell (PEMFC), is an energy conversion device that converts the chemical energy of hydrogen into electrical energy. A PEMFC has high operating efficiency and zero or low emission. These advantages make the fuel cell the best candidate for application in electrical power generation.

Nomenclatures

A	Surface area, m ²
A_M	Membrane cross section area, m ²
d_{GC}	Gas channel depth, m
F	Faraday's constant, C kg mol ⁻¹
F_A	Anode mass flow rate, kg s ⁻¹
F_C	Cathode mass flow rate, kg s ⁻¹
j^{ref}	Reference exchange current density, A m ⁻²
k	Thermal conductivity, W m ⁻¹ K ⁻¹
l_{GC}	Gas channel length, m
M_W	Molecular mass of species, kg kmol ⁻¹
R	Universal gas constant, J K ⁻¹ mol ⁻¹
$R_{an,cat}$	Volumetric transfer current in anode or cathode, A m ⁻³
$R_{sol,mem}$	Volumetric transfer current in solid or membrane, A m ⁻³
S_X	Species volumetric source term, kg s ⁻¹ m ⁻³
S_ϕ	Source of ϕ
t	Time, s
t_{CC}	Current collector thickness, m
t_{CL}	Catalyst layer thickness, m
t_{GDL}	GDL thickness, m
t_M	Membrane thickness, m
V	Volume, m ⁻³
V_{oc}	Open circuit voltage, V
w_{CC}	Current collector width, m
w_{GC}	Gas channel width, m
x_{H_2}	H ₂ mass fraction
x_{O_2}	O ₂ mass fraction
[i]	Molar concentration of species i , mol m ⁻³

Greek Symbols

α	Transfer coefficient
Γ_ϕ	Diffusivity coefficient of ϕ
γ	Concentration exponent
ε	Porosity
ζ	Specific active surface area, m ⁻¹
η	over-potential, V
$\sigma_{sol,mem}$	Electrical conductivity in solid/membrane, Ω^{-1} m ⁻¹
ϕ	Transported quantity
$\phi_{sol,mem}$	Electric potential in solid/membrane, V

Abbreviations

3D	Three dimensional
GDL	Gas diffusion layer
PEMFC	Proton exchange membrane fuel cell
PTFE	Polytetrafluoroethylene

Gas diffusion layers (GDLs) in a PEMFC are porous media that consist of a thin layer of carbon black mixed with polytetrafluoroethylene (PTFE) [1]. Several pivotal functions of a GDL such as it permeates gas and helps remove

by-product water that form during fuel cell operation [2]. It is shown that GDL properties, such as porosity and PTFE content, have a significant effect on fuel cell performance [1-3].

Previous studies report that GDL porosity affects the distribution of liquid water content and PEMFC performance [4]. The effect of GDL porosity was investigated by Sahraoui et al. [5]. They concluded that PEMFC performance decreases if GDL porosity decreases. This result is caused by the small sizes of the pores for gas diffusion and transportation.

The hydrophobicity of GDL is controlled by hydrophobic treatment to remove liquid water saturation in the cathode effectively. Hydrophobic agents, such as PTFE, should be added to increase the hydrophobicity of GDL [6]. This feature reduces the flooding of water in the GDL and provides the reactant access to the catalyst layer [7]. Experimental investigations were conducted by Ismail et al. [8] to measure the through-plane permeability of the GDL treated with and without PTFE. Their study showed that the highest performance of the GDL was observed at 5 wt% PTFE content. This finding indicated that the PTFE content did not necessarily result in the best performance of the PEMFC. The PTFE content in the GDL should be balanced and optimized to achieve the highest PEMFC performance.

The modeling and simulation of PEMFC performance by using commercial codes have been the focus of considerable attention in recent years. Modeling and simulation provide researchers with the ability to obtain an in-depth understanding of the underlying phenomena occurring within the fuel cell given the geometric parameters, material properties, and operating conditions [9] and to conduct design optimization [10] at a low cost.

A detailed literature review and comparison of approaches to PEMFC modeling was presented by Cheddie and Munroe [9] who discussed the three main categories of fuel cell models. Arvay et al. [11] simulated a full 3D evaluation of convergence by using realistic geometry and material parameters. Arvay et al. [11] stated that errors can arise from unrepresentative geometry, mesh dependency, mathematical model accuracy, discretization, and convergence errors.

In this study, we aim to develop a 3D model to numerically investigate the optimum GDL parameters, such as porosity and PTFE content, in PEMFC. The model was developed by using ANSYS FLUENT 14.5 with a built-in Fuel Cell and Electrolysis Module.

2. Model Development

The model presented in this study is a 3D single model. Figure 1 shows the schematic of the computational domain for the 3D PEMFC model that was developed by using the ANSYS Design Modeler. The top side of the model is the anode, whereas the bottom side of the model is the cathode. The model includes a proton exchange membrane, catalyst layers of the anode and cathode, GDLs of the anode and cathode, gas channels of the anode and cathode, and current collectors of the anode and cathode. The model adopted the straight path of a typical serpentine flow field pattern in the gas distributor plate of the PEMFC to avoid the high computation requirements in modeling the entire complex flow field.

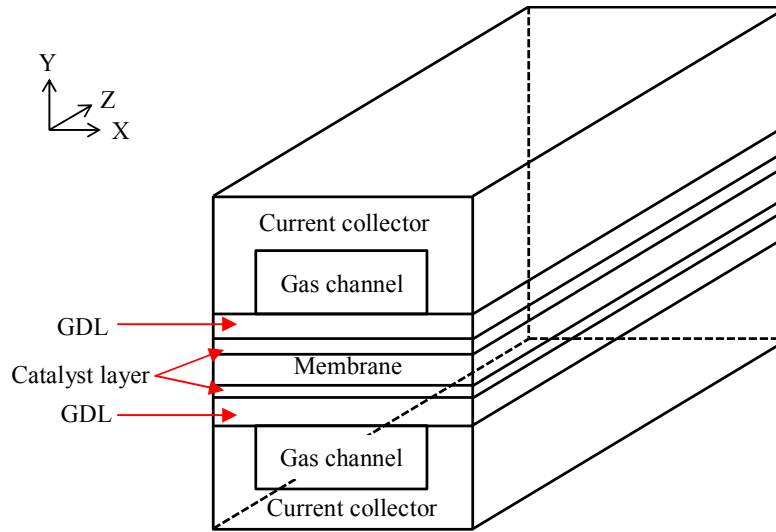


Fig. 1. Schematic diagram of the PEMFC model.

2.1. Model equations

The model equations discussed in this section are based on the ANSYS FLUENT Fuel Cell Module Manual [12]. The 3D fluid flow is solved by using the Navier–Stokes transport equation in its conservative form and can be written as follows:

$$\frac{\partial}{\partial t} \int_V \rho \phi dV + \oint_A \rho \phi \mathbf{V} \cdot d\mathbf{A} = \oint_A \Gamma_\phi \nabla_\phi \cdot d\mathbf{A} + \int_V S_\phi dV \quad (1)$$

where ϕ is the transported quantity, t is the time, A is the surface area, V is the volume, Γ_ϕ is the diffusivity coefficient, S_ϕ is the source of ϕ .

The surface over-potential is the driving force behind the reactions in the fuel cell, and the equations are solved as follows:

$$\nabla \cdot (\sigma_{sol} \nabla \phi_{sol}) + R_{sol} = 0 \quad (2)$$

$$\nabla \cdot (\sigma_{mem} \nabla \phi_{mem}) + R_{mem} = 0 \quad (3)$$

where $\sigma_{sol,mem}$ is the electrical conductivity of the solid or membrane, $\phi_{sol,mem}$ is the electric potential of the solid or membrane and $R_{sol,mem}$ is the volumetric transfer current in the solid or membrane.

The Butler–Volmer function is used to calculate the transfer currents within the catalyst layers:

$$R_{an} = \zeta_{an} i_{an}^{ref} \left(\frac{[H_2]}{[H_2]_{ref}} \right)^{\gamma_{an}} \left(e^{\alpha_{an} F \eta_{an} / RT} - e^{-\alpha_{cat} F \eta_{an} / RT} \right) \quad (4)$$

$$R_{cat} = \zeta_{cat} j_{cat}^{ref} \left(\frac{[O_2]}{[O_2]_{ref}} \right)^{\gamma_{cat}} \left(e^{\alpha_{an} F \eta_{cat} / RT} + e^{-\alpha_{cat} F \eta_{cat} / RT} \right) \quad (5)$$

where ζ is the specific active surface area and j^{ref} is the reference exchange current density per active surface area. The quantities in the brackets represent the local species concentration, γ is the concentration exponent, α is the transfer coefficient, F is Faraday's constant and R is the universal gas constant. The quantity η is the local surface over-potential or activation loss which is solved by using the following equations where V_{oc} is the open circuit voltage.

$$\eta_{an} = \phi_{sol} - \phi_{mem} \quad (6)$$

$$\eta_{cat} = \phi_{sol} - \phi_{mem} - V_{oc} \quad (7)$$

Source terms for chemical species (H_2 , O_2 , and H_2O) are added to account for the electrochemical reaction:

$$S_{H_2} = -\frac{M_{W,H_2}}{2F} R_{an} \quad (8)$$

$$S_{O_2} = -\frac{M_{W,O_2}}{4F} R_{cat} \quad (9)$$

$$S_{H_2O} = \frac{M_{W,H_2O}}{2F} R_{cat} \quad (10)$$

where S_X is the species volumetric source terms and M_W is the molecular mass of the species. The positive and negative signs indicate that hydrogen and oxygen are consumed and water is generated [11]. The current conservation induced by the total electric current produced in the catalyst layers is calculated by using the following equation:

$$\int_{anode} R_{an} dV = \int_{cathode} R_{cat} dV \quad (11)$$

2.2. Geometry, parameters and mesh generation

The physical parameters and dimensions of the PEMFC model are obtained on the basis of literature surveys. Table 1 shows the information on the physical parameters and dimensions of the model [13-14].

A grid independence study was conducted by generating the simulation under the same operating conditions and parameters but with different element sizes focused on GDLs only. Three different element sizes of 1×10^{-5} m (Mesh 1), 1×10^{-6} m (Mesh 2), and 1×10^{-7} m (Mesh 3) at GDLs were generated. All simulations presented in this study were conducted by using the finest grid. At a cell potential of 0.95 V, Mesh 1 and 3 yield deviations of approximately 1.31% and 0.17% for the average current density, respectively, compared to Mesh 2.

This finding indicated that Mesh 2 provides reasonably accurate results. Therefore, Mesh 2 is used in this study for further analysis.

Table 1. Parameters and dimension of the PEMFC model.

Parameter	Value
Membrane thickness, t_M	5.0×10^{-3} m
Catalyst layer thickness, t_{CL}	2.5×10^{-5} m
GDL thickness, t_{GDL}	2.0×10^{-4} m
Gas channel depth, d_{GC}	8.0×10^{-4} m
Current collector thickness, t_{CC}	1.2×10^{-3} m
Gas channel length, l_{GC}	5.0×10^{-2} m
Gas channel width, w_{GC}	2.0×10^{-3} m
Current collector width, w_{CC}	4.0×10^{-3} m
Cell temperature, T_C	343 K
Anode mass flow rate, F_A	1.0×10^{-6} kg s ⁻¹
H ₂ mass fraction, x_{H_2}	0.8
Cathode mass flow rate, F_C	1.0×10^{-5} kg s ⁻¹
O ₂ mass fraction, x_{O_2}	0.9
Membrane cross section area, A_M	0.002 m ²
Anode reference exchange current density, j_{an}^{ref}	30 A m ⁻²
Cathode reference exchange current density, j_{cat}^{ref}	4.0×10^{-3} A m ⁻²
Anode transfer coefficient, α_{an}	3
Cathode transfer coefficient, α_{cat}	3

Figure 2 shows the selected meshed model that was obtained by using ANSYS Meshing. The meshed model had 93,526 elements with structured hexahedral grids. The simulations were conducted by using ANSYS FLUENT 14.5 for the steady-state condition to investigate the optimum porosity and PTFE content of GDL by determining the current density produced at different operating voltages. The model assumed that only a laminar flow regime occurred in the gas channels and the GDLs and membrane were completely impervious to gases.

Table 2. Mesh parameters on each subcomponent of PEMFC model.

Mesh parameter	Current collectors	Gas channels	Gas diffusion layers	Catalyst layers	Membrane
Element size	0.0001 m	0.0001 m	1.0×10^{-6} m	1.0×10^{-6} m	1.0×10^{-7} m

The simulation cases were conducted by using the built-in Fuel Cell and Electrolysis Module in ANSYS FLUENT 14.5. This module is an interactive environment that allows users to key in the PEMFC parameters during the preprocessing stage. The calculation was conducted by using an Intel Core™ i7-3770 (3.4 GHz) CPU with 4 GB RAM in Windows OS 7 64-bit. Table 3 shows the spatial discretization settings that were implemented during the iteration process of the model in ANSYS FLUENT 14.5. The iteration process set the coupled scheme for the pressure–velocity coupling setting for the solution control of the model. In this study, the under-relaxation factors were set to 0.5 for the solution control of the model. These spatial discretization and under-relaxation

factor settings were observed to balance the iteration processes from divergence, further accelerating the iteration processes into the convergence criteria. The convergence absolute criteria were monitored and checked at 1×10^{-3} for all residuals of the equations, except for the energy that was checked at 1×10^{-5} .

Table 3. Spatial discretization setting in ANSYS FLUENT.

Spatial discretization	Method
Gradient	Least squares cell based
Pressure	Standard
Density	Second order upwind
Momentum	Second order upwind
Hydrogen	Second order upwind
Oxygen	Second order upwind
Water	Second order upwind
Energy	Second order upwind
Electric potential	First order upwind
Protonic potential	First order upwind
Water saturation	First order upwind
Water content	First order upwind

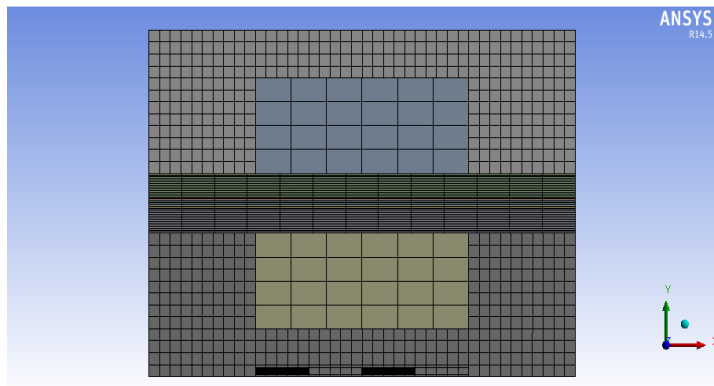


Fig. 2. Grid generation of the PEMFC model.

3. Results and Discussion

3.1. Porosity

Porosity values ε that have been studied were 0.2, 0.4, 0.6 and 0.8. These values were selected on the basis of literature surveys and were set on the anode and cathode sides of the GDL of the PEMFC. The simulation results in Fig. 3 show that fuel cell performance was higher at higher GDL porosity. These results were consistent with the results reported by Sahraoui et al. [5]. This study showed that PEMFC produced the best performance at a porosity value of 0.8 and the least performance at a porosity value of 0.2. The trend of the results for porosity values of 0.6 and 0.8 were similar between 0.2 and 0.4 V because the current densities produced were slightly different but higher at a porosity of 0.8.

The PEMFC with the lowest GDL porosity value of 0.2 had a high mass transfer resistance of reactants to the reaction sites because of the small pores in the GDL. This situation resulted in reduced reactant concentration. The PEMFC with the highest GDL porosity value had a low mass transfer resistance and had a consistent diffusion of reactants to the catalyst layer. At higher porosity, the distribution of hydrogen and oxygen gases is more uniform and easier to diffuse into the catalyst layer. Moreover, a high GDL porosity value facilitates the management of water produced as a by-product [14]. The produced water easily passes out of the PEMFC, thus providing adequate space for the reactants to diffuse into the reaction sites.

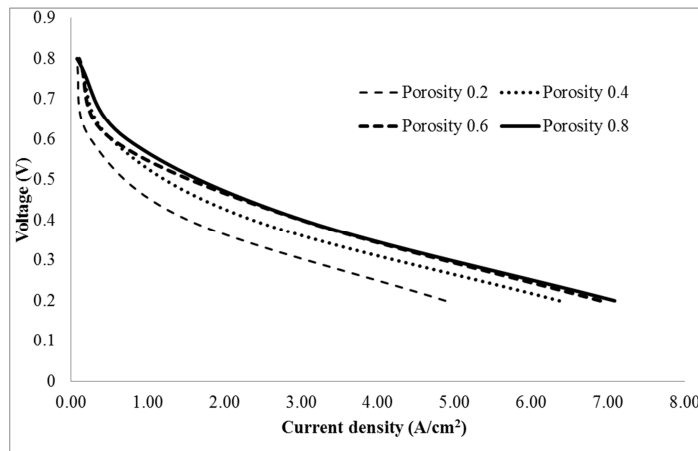


Fig. 3. Polarization curves for PEMFC with different GDL porosity values.

3.2. Polytetrafluoroethylene content

For the study of the different PTFE contents in GDL, GDL commercial data that can be acquired from the market were used as reference. The type of GDL acquired must be from the same GDL manufacturer to obtain precise results. This study used the SIGRACET[®] 24 series, namely, SIGRACET[®] GDL 24 AA (0 wt% PTFE), SIGRACET[®] GDL 24 BA (5 wt% PTFE) and SIGRACET[®] GDL 24 DA (20 wt% PTFE), from the SGL Group SIGRACET[®] to ensure a constant GDL thickness. Different numbers of SIGRACET[®] GDL indicate different thicknesses [15]. Data obtained from Sadeghifar et al. [15] and Pfrang et al. [16] were used in this study (Table 4).

Table 4. Specifications of SIGRACET[®] GDL 24 series [15, 16].

SIGRACET [®] GDL 24	AA	BA	DA
PTFE (wt%)	0	5	20
PTFE thickness on each surface (μm)	0	1.5	3
Porosity, ε (%)	88	84	72
Thickness (μm) \pm 5	190	190	190
Thermal conductivity, k ($\text{W m}^{-1} \text{K}^{-1}$)	0.48	0.31	0.22
Electrical resistance ($\text{m}\Omega \text{cm}^{-2}$)	5	10	12

Figure 4 shows the polarization curves from the simulations with different PTFE contents. On the basis of this result, the optimum PTFE content in the GDL that produced the best PEMFC performance is SIGRACET® GDL 24 BA, which contains 5 wt% PTFE, whereas the lowest PEMFC performance is SIGRACET® GDL 24 DA, which contains 20 wt% PTFE. The results obtained were consistent with the results of the studies of Ismail et al. [8], who reported that the optimum PTFE content in the GDL is 5 wt%.

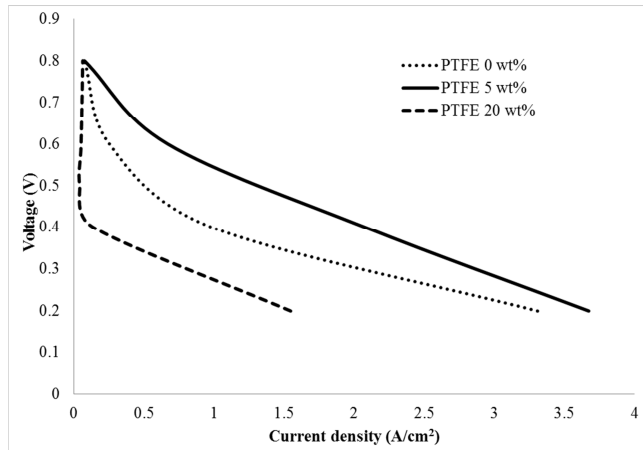


Fig. 4. Polarization curves for PEMFC with different PTFE contents.

The main purpose of adding PTFE in the GDL is to assist in water management and to reduce water flooding [7]. Different PTFE contents in the GDL result in different effects, which affect PEMFC performance. A higher PTFE content does not necessarily result in high performance or otherwise. A higher PTFE content in the GDL corresponds to more hydrophobic GDL characteristics. This phenomenon minimizes the potential of GDL to experience water flooding. Therefore, the decrease in reactant concentration because of water flooding can be reduced by increasing the PTFE content in the GDL.

However, improving the PTFE content in the GDL also reduces the electrical conductivity, porosity, and gas permeability of the GDL [6]. A high PTFE content can reduce the size of the GDL pores, thus affecting gas permeability. Moreover, this phenomenon increases the electrical resistance in the GDL, and then results in lower PEMFC performance. Therefore, the optimum PTFE content should be set for better PEMFC performance [8]. The PTFE content should not be too high such that it does not increase the electrical resistance and decrease the GDL porosity. The PTFE content should not be too low such that water in the PEMFC can be managed efficiently.

4. Conclusions

Studies on the effects of changes in the GDL porosity showed that a high porosity helps enhance the performance of PEMFC. A porous GDL increased the mass transfer of fuel and the amount of fuel involved in the electrochemical reaction.

Studies on the effects of PTFE content, which differ from GDL porosity, showed that the highest PTFE content did not necessarily result in high performance or otherwise. Thus, the PTFE content in the GDL should be optimized to help remove the water. The results of this study were consistent with the results of other investigations in published literature who reported that the optimum PTFE content in the GDL was approximately 5 wt%.

Acknowledgement

The authors acknowledge Universiti Kebangsaan Malaysia and Ministry of Education Malaysia for funding this research work through grants GGPM-2012-084 and FRGS/1/2013/TK07/UKM/02/1.

References

1. Jordan, L.R.; Shukla, A.K.; Behrsing, T.; Avery, N.R.; Muddle, B.C.; and Forsyth, M. (2000). Diffusion layer parameters influencing optimal fuel cell performance. *Journal of Power Sources*, 86(1–2), 250-254.
2. Didari, S.; Harris, T.A.L.; Huang, W.; Tessier, S.M.; and Wang, Y. (2012). Feasibility of periodic surface models to develop gas diffusion layers: A gas permeability study. *International Journal of Hydrogen Energy*, 37(19), 14427-14438.
3. Lee, H.-K.; Park, J.-H.; Kim, D.-Y.; and Lee, T.-H. (2004). A study on the characteristics of the diffusion layer thickness and porosity of the PEMFC. *Journal of Power Sources*, 131(1–2), 200-206.
4. Yan, W.-M.; Hsueh, C.-Y.; Soong, C.-Y.; Chen, F.; Cheng, C.-H.; and Mei, S.-C. (2007). Effects of fabrication processes and material parameters of GDL on cell performance of PEM fuel cell. *International Journal of Hydrogen Energy*, 32(17), 4452-4458.
5. Sahraoui, M.; Kharrat, C.; and Halouani, K. (2009). Two-dimensional modeling of electrochemical and transport phenomena in the porous structures of a PEMFC. *International Journal of Hydrogen Energy*, 34(7), 3091-3103.
6. Park, S.; Lee, J.-W.; and Popov, B.N. (2012). A review of gas diffusion layer in PEM fuel cells: Materials and designs. *International Journal of Hydrogen Energy*, 37(7), 5850-5865.
7. Daino, M.M.; and Kandlikar, S.G. (2012). 3D phase-differentiated GDL microstructure generation with binder and PTFE distributions. *International Journal of Hydrogen Energy*, 37(6), 5180-5189.
8. Ismail, M.; Damjanovic, T.; Hughes, K.; Ingham, D.; Ma, L.; Pourkashanian, M.; and Rosli, M. (2010). Through-plane permeability for untreated and PTFE-treated gas diffusion layers in proton exchange membrane fuel cells. *Journal of Fuel Cell Science and Technology*, 7(5), 051016.
9. Cheddie, D.; and Munroe, N. (2005). Review and comparison of approaches to proton exchange membrane fuel cell modeling. *Journal of Power Sources*, 147(1–2), 72-84.

10. Iranzo, A.; Muñoz, M.; Rosa, F.; and Pino, J. (2010). Numerical model for the performance prediction of a PEM fuel cell. Model results and experimental validation. *International Journal of Hydrogen Energy*, 35(20), 11533-11550.
11. Arvay, A.; Ahmed, A.; Peng, X.H.; and Kannan, A.M. (2012). Convergence criteria establishment for 3D simulation of proton exchange membrane fuel cell. *International Journal of Hydrogen Energy*, 37(3), 2482-2489.
12. ANSYS FLUENT 14.5 Fuel Cell Modules Manual. Canonsburg, PA: ANSYS, Inc.; 2012.
13. Rismanchi, B.; and Akbari, M.H. (2008). Performance prediction of proton exchange membrane fuel cells using a three-dimensional model. *International Journal of Hydrogen Energy*, 33(1), 439-448.
14. Wei, Y.; and Zhu, H. (2011). Model and simulation of proton exchange membrane fuel cell performance at different porosity of diffusion layer. *International Journal of Modern Education and Computer Science (IJMECS)*, 3(2), 22.
15. Sadeghifar, H.; Djilali, N.; and Bahrami, M. (2014). Effect of Polytetrafluoroethylene (PTFE) and micro porous layer (MPL) on thermal conductivity of fuel cell gas diffusion layers: Modeling and experiments. *Journal of Power Sources*, 248, 632-641.
16. Pfrang, A.; Veyret, D.; and Tsotridis, G. (2011). Computation of thermal conductivity of gas diffusion layers of PEM fuel cells. *Convection and Conduction Heat Transfer*, 10, 232-215.